ICCAUA Proceedings Journal
Proceedings of the international conference of contemporary affairs in architecture and urbanism-ICCAUA
Volume 9 (December 2026), 2610296

Journal homepage: https://journal.iccaua.com/

ICCAUA Proceedings Journal

DOI: https://doi.org/10.38027/ICCAUA2026EN0296

Dual Functionality of Silica Fume in Very-High-Strength Heat-Resistant Concrete

*** [1] Zhwan Anwar Noori , [2] Ferhad Rahim Karim , [3] Hardy Kamal Karim**
[1,2, & 3] Department of Civil Engineering, college of Engineering, University of Sulaimani, Al-Sulaimanyah, Iraq
[1] E-mail: zhwan.noori@univsul.edu.iq, [2] E-mail: ferhad.karim@univsul.edu.iq, [3] E-mail: hardy.karim@univsul.edu.iq

Received: 28.04.2026
Revised: 28.06.2026
Accepted: 01.07.2026
Available online: 10.07.2026

This article has been selected and peer-reviewed for publication in this journal as part of the 9th International Conference of Contemporary Affairs in Architecture and Urbanism, held on 7–8 May 2026 in Istanbul, Türkiye.

Abstract

Very-high strength heat-resistant concrete (VHSHRC) is intended to withstand high temperatures without significantly degrading its characteristics. This research highlights the effect of silica fume on the properties of VHSHRC, and it was employed as a partial substitute for Portland cement at various ratios of 11.5%, 12%, 12.5%, and 13%. The properties, such as compressive and split tensile strength, bulk dry density, and water absorption, were measured under normal and different heating temperatures and durations. 165 cubes were used to determine compressive strength, and 150 specimens were examined for split tensile strength, bulk dry density, and water absorption. The results show that the optimal silica fume replacement ratio in VHSHRC was 12.5%, resulting in a 3.72% increase in compressive strength at 125°C and a 32.18% reduction in water absorption due to the improvement in pozzolanic reaction by silica fume and its ability to reduce the number and size of micro-pores.
Keywords: Bulk dry density; Compressive strength; Split tensile strength; Silica fume; Very-high strength heat-resistant concrete; Water absorption.

1. Introduction

1.1 Background

The exceptional mechanical properties, cost-effectiveness, durability, and efficiency of concrete make it essential in high-rise buildings (Kulkarni, 2016; Tanash et al., 2024). Very-High Strength Concrete (VHSC) generally refers to concrete having a cylinder compressive strength of more than 70 MPa (10,000 psi) at 28 days for cylindrical samples having 100 × 200 mm, and the tensile to compressive strength ranging from 8% to 12%. The water-to-binder ratio of this type of concrete is usually less than 0.35. The VHSC has been employed in high-rise structures and various concrete applications (Gernay et al., 2021; Hilal, 2016; Mehta & Monteiro, 2014; Yang & Hwang, 2017; Zia et al., 1993).

Heat-resistant concrete (HRC) is a special kind of concrete specifically designed to withstand raised temperatures without showing remarkable degradation in its mechanical properties. Therefore, this type of concrete is widely employed in specific structures that are subjected to high temperatures, including furnaces, chimneys, fireplaces, kilns, incinerators, and other industrial structures (Dvorkin et al., 2022; Otakulov et al., 2021).

Very-High Strength Heat-Resistant Concrete (VHSHRC) is a distinctive type of concrete that possesses both very- high strength and high thermal resistance under load. Hence, this kind of concrete has a wide application in structures that endure significant mechanical and thermal loads, such as fire-prone high-rise buildings, defense structures, tunnels, power plants, and industrial furnaces. Moreover, this type of concrete has the capability to maintain its durability under elevated temperatures (Bao et al., 2023; Chen et al., 2023).

The global demand for reusing construction waste materials such as RAP aggregate in concrete buildings has gained significant attention, as an attempt to reduce the amount of waste materials accumulated pressing environmental issues and the necessity to produce sustainable, cost-effective buildings. On the other hand, current research studies acknowledge that incorporating RAP aggregate in concrete typically results in strength loss, due to the asphalt binder coating the RAP aggregate particles that weakens the interfacial transition zone (ITZ) of the concrete matrix, specifically at replacement ratios exceeding 10% (Abedalqader et al., 2021; Jaawani et al., 2021; Noori et al., 2025, 2026).

The inclusion of supplementary cementitious materials (SCM) as a partial replacement of cement in concrete production provides a reduction in the quantity of cement production and carbon dioxide emissions. The SCMs include Fly ash, Metakaolin, SF, blast-furnace slag, and rice husk ash. Furthermore, these materials enhance the properties of concrete in terms of mechanical and non-mechanical qualities through the dual effect of pozzolanic activity and filling effect (Karim, 2024). Therefore, they find their applications in the manufacture of very-high strength concrete that requires very high mechanical strength with maintained durability (Knight et al., 2023; Nadeem et al., 2014).

The influence of SF on the compressive strength of High-Strength Concrete (HSC) under standard conditions and at elevated temperatures of 100°C, 200°C, 300°C, and 600°C for three hours was investigated. The SF was added as a partial replacement of cement with dosages of 6% and 10%. The residual relative compressive strengths declined to 84.1%, 85.2%, 68.7%, and 26.8% at heating temperatures of 100°C, 200°C, 300°C, and 600°C, respectively, for the concrete mix incorporated 10% SF compared to its unheated state. Additionally, the rate of strength loss increased with higher SF content, indicating that SF addition had not effectively mitigated heat-induced stresses (Behnood & Ziari, 2008; Ghandehari et al., 2010).

Previous investigations revealed that the inclusion of SF yielded higher compressive strength than the control mix when exposed to elevated temperatures. Nevertheless, among concretes that contain SF, reductions in compressive strength are noticed compared with their unheated condition. The reduction in compressive strength of HSC begins at approximately 100°C, and severe strength loss was detected beyond 200°C (Albeer & Hassan, 2023; Behnood & Ziari, 2008; Elmesiri et al., 2022; Ghandehari et al., 2010; Ibrahim, 2016). As the temperature increased, the compressive strength decreased. This decline is primarily associated with thermally induced degradation and spalling of concrete due to breakdown of calcium silicate hydrate phases, and development of micro-cracks. Consequently, SF contributes to improved strength relative to the control, but its positive contribution is lost at raised temperatures. This early-stage strength loss remains a major concern and has not been adequately addressed.

Under different thermal exposure, for HSC that contain SF, reductions in split tensile strength were observed compared to their unheated condition. The reduced strength is related to accelerated degradation of the cementitious compound by heat exposure and micro-crack propagation within the microstructure. However, for NSC, the inclusion of SF contributed to enhanced compressive strength compared to their unheated state (Elmesiri et al., 2022).

1.2 Significance of the research

This research highlights the inflection point for using Silica fume (SF) to work in VHSHRC as a binder or as an inert filler to enhance some of the mechanical properties and non-mechanical properties as well under the effect of heating based on the Silica fume quantity in the concrete.

2. Materials and Methods

The incorporation of SF into VHSHRC at different rates of 11.5%, 12%, 12.5%, and 13% to assess the effect of SF on some of the mechanical and non-mechanical tests of the concrete, to explain its effect as a binder, and how this pozzolanic material works as a filler. The tests were performed under both standard laboratory conditions and different elevated temperatures of 125°C, 150°C, and 175°C with various heating durations of 2, 4, and 6 hours.

2.1 Selection of materials

The selection of materials for this study includes Portland cement, fine aggregates, SF, and admixture; their properties were adopted from a previous study currently under publication (Noori et al., 2025).

2.1.1 Portland cement

For this study, Ordinary Portland cement was selected throughout the research, and it lies within the ASTM specifications of ASTM C150-20 (ASTM, 2018, 2020c). Moreover, the properties of the used cement are tabulated in Table 1.

Table 1: Physical properties of Portland cement utilized in the study, ASTM C150-20.

Physical properties	Results	Allowable limit
Average cube compressive strength, MPa at the age of 7 days	23.65	19 MPa
Normal consistency, %	33.2	-
Initial setting time, minutes	130	Minimum 45
Final setting time, minutes	246	Maximum 375
Specific gravity	3.1	3.1-3.14

2.1.2 Silica fume

Silica fume was selected as a pozzolanic material and incorporated as SCM in VHSHRC production with a particle size of 0.15 micron. The silica content in SF plays a vital role in reacting with calcium hydroxide. The percentage of silica in SF used in this research is 98.41%.

2.1.3 Fine aggregates

In the production of VHSHRC, three kinds of fine aggregate were used, including quartz sand, magnetite black sand, and RAP aggregate. Furthermore, the quantities and properties of the three types of aggregate are based on a previous study (Noori et al., 2025), as shown in Table 2. The quartz sand is used because it can withstand high temperatures, as it contains more than 90% of silicon dioxide. In addition, magnetite black sand is used owing to its capability to endure elevated temperatures and maintain the relative residual strength of VHSHRC. The source of RAP aggregate and the preparation method of RAP aggregate were adopted from (Noori et al., 2025). The chemical composition of the RAP aggregate and magnetite black sand is presented in Table 3.

Table 2: Physical properties of fine aggregate.

Physical properties	Quartz sand	Magnetite black sand	RAP aggregate
Appearance/color	Granular/light tan	Granular/black	Granular/brown
Water absorption, %	0.32	0.65	2.389
Bulk specific gravity	2.6	4.789	2.513
Particle size, mm	0.3-0.7	0.15-0.4	0.15-0.43
Fineness modulus	2.53	1.01	1.47

Table 3: Chemical composition of RAP aggregate and magnetite black sand.

Chemical composition	Quantity, %	
	RAP aggregate	Magnetite black sand
SiO_2	34.74	0.15
CaO	31.98	-
Fe_2O_3	3.12	-
Fe_3O_4	-	99.45
Al_2O_3	4.634	0.27
LOI	22.41	-
Others	3.116	0.13

2.1.4 Admixture

To increase the workability and enhance the strength of VHSHRC mixes, a special kind of high-range water-reducing admixture is used, which is Polycarboxylate-based, namely (Sika Viscocrete 1681). The specific gravity and pH value of the admixture are 1.070 and 5.5, respectively. The mash cone test was performed, which assesses the dosage of admixture, obtaining desired workability and strength of concrete (Kumar et al., 2024; Roussel, 2006). A total of 10 trials were made, with superplasticizer dosages starting from 1.2% to 1.6% of the weight of cement; the optimum dosage of superplasticizer to cement was 1.53%.

2.1.5 Mixing Water

Warm potable water was used for preparing all concrete mixes, which were free from clay, organic, or harmful substances. The mixing water lies within acceptable limits for use in the production of concrete with total dissolved solids of 200-230 mg/L and electrical conductivity of 400-430 µS/cm.

2.2 Mix Proportions

The mix proportions of the VHSHRC mix were based on previous research on VHSHRC, which investigated the mechanical properties of the concrete by incorporating RAP aggregate (Noori et al., 2025). The concrete mix with optimum RAP content was selected as the control mix. For the control mix with an admixture to cement ratio of 0.015, water to cement ratio of 0.21, and total sand to cement ratio of 0.912. The total fine sand is mainly composed of quartz sand, then magnetite black sand was introduced as a partial replacement of quartz sand, and the final ratio of magnetite black sand to quartz sand was 0.31. After that, RAP aggregate was used as a partial substitution for the remaining silica sand. The ratio of RAP aggregate to quartz sand was 0.05.

Initially, SF was incorporated into VHSHRC at 8% - 20% as a partial replacement of cement. Flow table test and setting time were performed to evaluate the workability of VHSHRC mixes for all ratios of SF according to (ASTM, 2014, 2019). The result of the flow table test was more than 105% for mixes containing 8%, 10%, 12%, and 14% of SF, except for mixes containing 16% of SF, in which the value was less than 105%. Besides, the setting time was less than 45 minutes for mixes containing 14%, 16%, 18% and 20% of SF. Hence, the upper limit of SF that satisfies the workability criteria was 14%.

Moreover, to determine the lower limit of SF in the mix, cube compressive strength was performed at the age of 7 days for all SF contents, and the concrete mixes having strengths lower than 85 MPa were excluded. For concrete mixes that contain 8% and 10% of SF, the compressive strength was less than the targeted strength. Ultimately, four SF ratios were selected based on the required workability and targeted strength, in which the flow spread value exceeded 105%, and the setting time was more than 45 minutes for mixes containing different replacement percentages of cement with SF at 11.5%, 12%, 12.5%, and 13%. The methodology of the research is summarized in Table 4.

Table 4: Summary of the experimental program, including the number of samples to perform the tests.

Tests	Heating temperature	Heating duration, hours	Number of samples				
			Quantity of SF in VHSHRC				
			0%	11.5%	12%	12.5%	13%
Compressive strength	20°C	-	6	3	3	3	3
	125°C	2	3	3	3	3	3
		4	3	3	3	3	3
		6	3	3	3	3	3
	150°C	2	3	3	3	3	3
		4	3	3	3	3	3
		6	3	3	3	3	3
	175°C	2	3	3	3	3	3
		4	3	3	3	3	3
		6	3	3	3	3	3
Split tensile strength	20°C	-	3	3	3	3	3
	125°C	2	3	3	3	3	3
		4	3	3	3	3	3
		6	3	3	3	3	3
	150°C	2	3	3	3	3	3
		4	3	3	3	3	3
		6	3	3	3	3	3
	175°C	2	3	3	3	3	3
		4	3	3	3	3	3
		6	3	3	3	3	3
Water absorption	20°C	-	3	3	3	3	3
	125°C	2	3	3	3	3	3
		4	3	3	3	3	3
		6	3	3	3	3	3
	150°C	2	3	3	3	3	3
		4	3	3	3	3	3
		6	3	3	3	3	3
	175°C	2	3	3	3	3	3
		4	3	3	3	3	3
		6	3	3	3	3	3
Bulk dry density	20°C	-	3	3	3	3	3
	125°C	2	3	3	3	3	3
		4	3	3	3	3	3
		6	3	3	3	3	3
	150°C	2	3	3	3	3	3
		4	3	3	3	3	3
		6	3	3	3	3	3
	175°C	2	3	3	3	3	3
		4	3	3	3	3	3
		6	3	3	3	3	3

3. Properties of VHSHRC at the hardened state

In its hardened condition, VHSHRC exhibits numerous physical and mechanical properties that affect the performance and longevity of the concrete. This study conducted several experiments at the age of 28 days to assess the mechanical and non-mechanical characteristics of VHSHRC. These assessments offer a thorough comprehension of the impact of SF on the performance of VHSHRC mixes.

3.1 Mechanical properties of the VHSHRC

At the hardened state, two tests were performed, including the cube compressive strength and split tensile strength tests. The tests were conducted for VHSHRC mixes at the age of 28 days, cured by a water bath for both the control mix and concrete mixes containing different ratios of SF.

3.1.1 Cube compressive strength

Standard cube specimens with 50 side length were tested. For the control mix and unheated samples, six samples were tested. For heated specimens, three samples were tested, and the average cube compressive strength was determined. The test was conducted according to ASTM C109 (ASTM, 2020a) with a loading rate of 0.2-1.0 MPa/s and a head movement rate of 1.3 mm/min ± 0.5 mm/min.

3.1.2 Split tensile strength

Standard cylinders with a diameter of 50 mm and a height of 100 mm were prepared and examined at the age of 28 days. The test was done as per ASTM C496 (ASTM, 2020b) with a loading rate of 0.017-0.023 MPa/s. For each condition, three samples were tested, and the average split tensile strength of the concrete was determined. Figure 1 shows the failure of concrete samples after the compressive and split tensile strength tests.

(a) Failure mode of the concrete cube after the compressive strength test

(b) Failure in a concrete cylinder after the split tensile strength test

Figure 1. Failure of concrete samples after subjecting them to compressive and split tensile loads.

3.2 Non-Mechanical Properties of VHSHRC

The non-mechanical properties of VHSHRC show a valuable insight into the durability via the incorporation of SF. In this investigation, the non-mechanical tests were conducted, including water absorption and bulk dry density.

3.2.1 Water Absorption

Standard concrete cube specimens with a side length of 100 mm were cast to determine the water absorption at the age of 28 days. Three samples were tested, and the average water absorption was determined according to BS1881-122:2011+A1:2020 (BS, 2020), as shown in Figure 2.

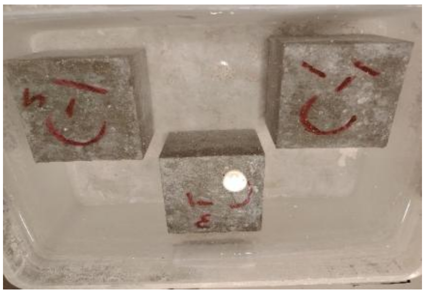

Figure 2. Concrete cube specimens immersed in water during the water absorption test.

3.2.2 Bulk Dry Density of Hardened Concrete

According to BS EN 12390-7:2019 (BSI, 2019), standard cube specimens with 50 mm side lengths were tested at the age of 28 days to determine the bulk dry density of VHSHRC. Three samples were tested, and the average value of the bulk dry density of hardened VHSHRC was determined. The bulk dry density was calculated by dividing the mass of the sample by its volume.

4. Results and Discussion

The experimental results of using SF as a binder and filler in VHSHRC to improve the properties of the concrete, even under elevated temperatures. The role of SF as a binder improves the mechanical properties, while the non-mechanical properties are enhanced through the filling effect of SF particles. The experimental program of the research comprised some of the mechanical and non-mechanical tests under both standard conditions and different elevated temperatures and durations.

4.1 Properties of the VHSHRC at the Fresh State

The flow table test and setting time of the concrete with different rates of SF were conducted according to (ASTM, 2014, 2019), as tabulated in Table 5.

Table 5: Flow values and setting time of VHSHRC at different SF replacement ratios.

Quantity of SF in VHSHRC, %	Flow, %	Setting time, minutes
0	Full flow	50
11.5	110	48
12	108	48
12.5	107	47
13	106	45

4.2 Mechanical Properties

The mechanical tests included compressive and split tensile strengths at both standard conditions and exposing the VHSHRC to different elevated temperatures of 125°C, 150°C, and 175°C. At each heating temperature, the concrete was maintained at the specified temperature for 2, 4, and 6 hours.

4.2.1 Cube Compressive Strength

For the standard conditions, using 12.5% SF in VHSHRC improves the compressive strength up to 111.1 MPa, due to the pozzolanic reaction and pore refinement by SF particles. Incorporation of a higher replacement ratio of SF reduced the compressive strength by 23.08% due to the excess amount of SF particles that work as fine aggregate rather than cementitious material, leading to increased water demand, and weakening the ITZ, thereby reducing compressive strength. While VHSHRC is subjected to 125°C, using 12.5% SF improves the compressive strength for all heat exposure durations, with the compressive strength improving by 3.72% after 6 hours of heat exposure compared to the mix without SF, due to a refined pore structure by high pozzolanic reaction and filling thermal micro-cracks by SF particles.

While VHSHRC was exposed to heating temperatures of 150°C and 175°C, the mix without SF shows the maximum compressive strength, followed by the mix containing 12.5% SF. The reason behind this reduction in the compressive strength of SF-concrete mixes is related to water vapor being trapped and producing internal pore pressure, leading to increased micro-cracks and compressive strength loss. The results of the compressive strengths with different ratios of SF are tabulated in Table 6.

Table 6: Compressive strength of VHSHRC at different ratios of SF under various elevated temperature conditions.

Quantity of SF, %	Compressive strength, MPa									
	20°C	125°C			150°C			175°C		
		Duration of heating, hours			Duration of heating, hours			Duration of heating, hours		
		2	4	6	2	4	6	2	4	6
0	110.71	89.40	90.57	91.48	98.56	106.34	118.14	106.71	111.08	131.33
11.5	93.82	84.72	84.99	86.39	90.61	91.79	99.06	91.23	95.50	97.94
12	94.49	89.86	90.70	94.28	92.17	94.48	99.68	92.15	95.57	98.70
12.5	111.10	91.25	92.21	94.88	95.02	102.31	103.47	96.08	99.29	110.77
13	85.16	81.01	81.87	82.32	87.68	91.26	95.02	84.39	85.09	99.50

4.2.2 Split Tensile Strength

At the standard condition, using SF at 12.5% shows a minimal reduction of 14.21% in the split tensile strength of VHSHRC, due to the action of SF that is limited to its filling effect rather than contributing as a cementitious material to improve the split tensile strength of concrete. In addition, under elevated temperatures, the inclusion of 12.5% SF drops the split tensile strength of VHSHRC up to 13.2%, 6.11%, and 19.88% compared to the mix without SF at the heating temperature of 125°C, 150°C, and 175°C for 6 hours, respectively, due to the filling effect of SF particles that work in restricting the release of combined water. Consequently, trapped water vapor generates high internal pore pressure, micro-crack formation, and strength loss. The results of the split tensile strength of VHSHRC are tabulated in Table 7.

Table 7: Split tensile strength of VHSHRC at different ratios of SF under various elevated temperature conditions.

Quantity of SF, %	Split tensile strength, MPa									
	20°C	125°C			150°C			175°C		
		Duration of heating, hours			Duration of heating, hours			Duration of heating, hours		
		2	4	6	2	4	6	2	4	6
0	12.222	10.983	10.216	10.716	9.936	10.954	11.671	10.066	10.538	13.202
11.5	9.395	8.689	9.032	9.253	8.687	9.039	9.125	9.333	9.812	10.779
12	9.402	9.496	8.163	8.943	10.361	10.219	9.993	10.372	9.942	8.817
12.5	10.485	9.653	9.696	9.301	10.432	10.454	10.958	10.412	10.023	10.578
13	8.277	8.987	8.825	8.649	9.073	8.817	9.439	8.849	8.598	9.692

4.3 Non-Mechanical Properties of VHSHRC

To evaluate the durability-related properties and to determine the quality of concrete, non-mechanical tests were performed, such as water absorption and bulk dry density. Beyond the mechanical and non-mechanical tests, microstructural analyses, including Field Emission Scanning Electron Microscopy (FESEM) and Energy-Dispersive X-ray Spectroscopy (EDS), were carried out to relate the microstructural characteristics of VHSHRC.

4.3.1 Water Absorption of Hardened Concrete

The partial replacement of cement with SF in VHSHRC causes filling of the micro-cracks and voids in concrete. Consequently, the water absorption reduces by 65.4% with the inclusion of 11.5% SF in VHSHRC, at standard conditions, as depicted in Figure 3. While VHSHRC samples subjected to heating at 125°C, 150°C, and 175°C, the inclusion of SF significantly reduces the water absorption of VHSHRC under all heat exposure conditions. Specifically, the water absorption reduces by 60.07%, 45.39%, and 34.19%, respectively, at heating temperatures of 125°C, 150°C, and 175°C for 6 hours, for concrete containing 11.5% SF compared to the mix without SF due to the role of very fine SF particles in filling thermal micro-cracks and producing denser microstructure. These effects contributed to reducing the connectivity of the capillary pores, thereby reducing the water ingress and reducing water absorption, as presented in Figures 4 and 5.

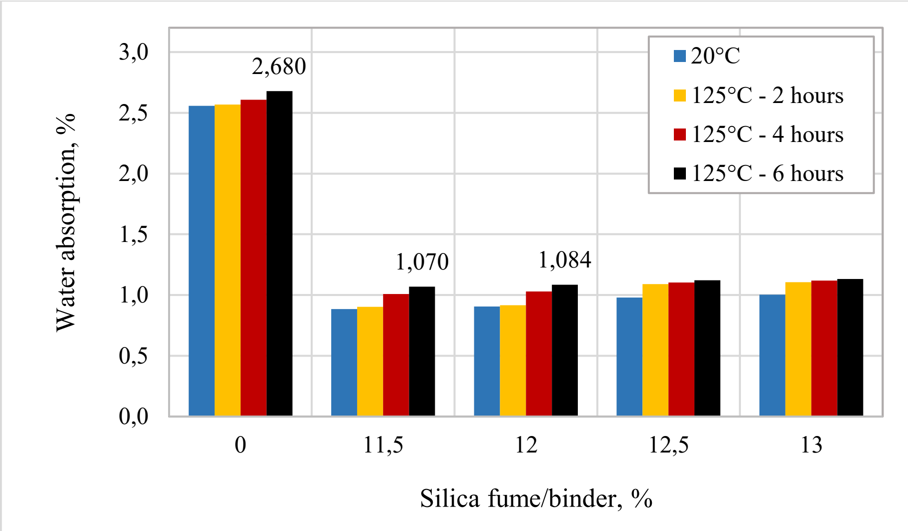

Figure 3. Effect of the SF amount on the water absorption of VHSHRC at standard conditions and at heating temperature of 125°C.

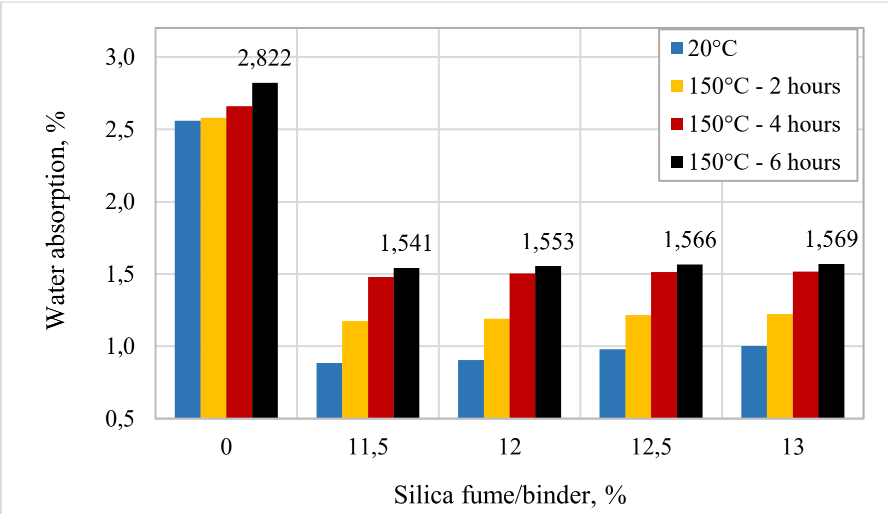

Figure 4. Effect of the SF amount on the water absorption of VHSHRC subjected to heating at 150°C.

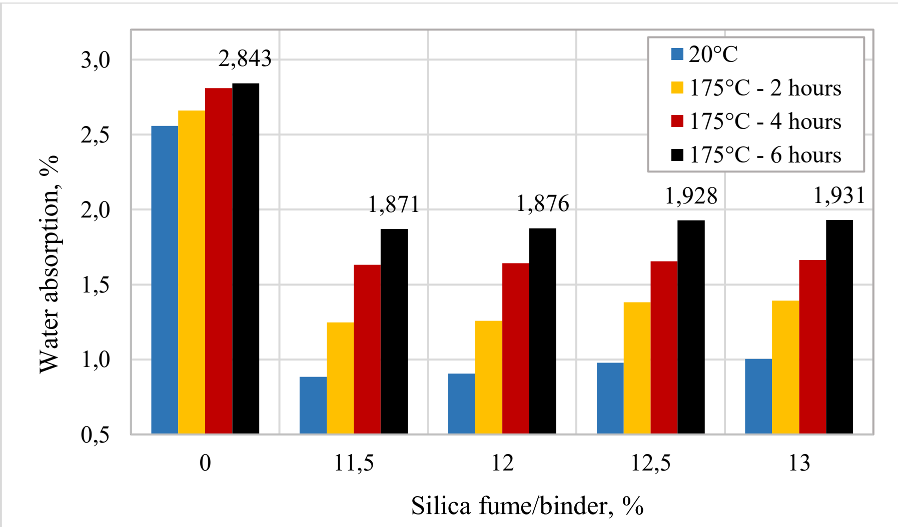

Figure 5. Effect of the SF amount on the water absorption of VHSHRC subjected to heating at 175°C.

4.3.2 Bulk Dry Density of the Hardened Concrete

The addition of SF into VHSHRC causes a reduction of 8.41%, 5.13%, 6.91%, and 7.7% in bulk dry density at 20°C, 125°C, 150°C, and 175°C, respectively, compared to concrete without SF due to the ultra-fine particle size and high surface area of SF particles, which increases the water demand that produces more small pores, contributing to the reduction of the bulk dry density under unheated and different elevated temperatures. However, among the mixes that contain SF, the concrete mix containing 12.5% SF exhibits maximum bulk dry density due to the maximum particle packing of fine aggregate within the cementitious matrix at unheated and all heated conditions, as shown in Table 8.

Table 8: Bulk dry density of VHSHRC incorporating SF at different replacement ratios under various elevated temperature conditions.

Quantity of SF,%	Bulk dry density, kg/m³									
	20°C	125°C			150°C			175°C		
		Duration of heating, hours			Duration of heating, hours			Duration of heating, hours		
		2	4	6	2	4	6	2	4	6
0	2498	2457	2454	2375	2443	2390	2346	2385	2342	2338
11.5	2256	2255	2246	2243	2229	2190	2182	2179	2171	2135
12	2282	2229	2225	2146	2228	2197	2141	2151	2149	2147
12.5	2288	2258	2255	2253	2236	2200	2184	2183	2183	2158
13	2220	2197	2190	2156	2177	2168	2156	2174	2146	2128

4.3.3 Microstructural Analyses of VHSHRC at the Different Heating Temperatures

The FESEM of VHSHRC shows minor localized heterogeneity at a heating temperature of 125°C; an increase in micro-cracks and micro voids within the concrete matrix is observed, due to the evaporation of free and combined water by the heating process, as shown in Figure 6b. Moreover, a pronounced reduction in Silicon from 24.05% to 18.08% and Calcium from 32.27% to 30.36% is observed, as tabulated in Table 9. While VHSHRC is exposed to an elevated temperature of 150°C, partial enhancement is observed by the formation of C–S–H within an increase of Silicon and Calcium, as shown in Figure 6c. The microstructural improvement of VHSHRC becomes more pronounced with extended heating of the concrete samples at 175°C, owing to increasing Silicon and Calcium to 24.91% and 44.62%, respectively, due to the secondary hydration that is facilitated by the remaining combined water with the softening of the asphalt binder coating. RAP aggregates particles as shown in Figure 6d.

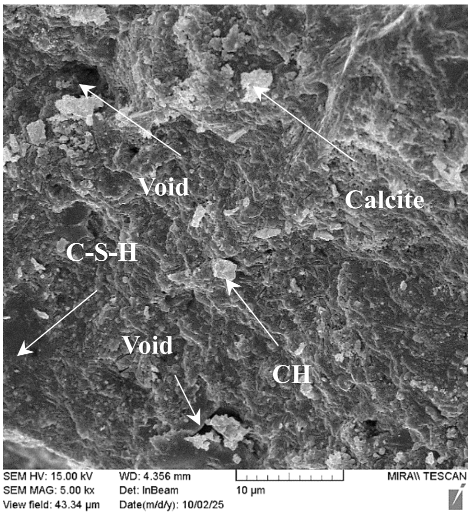

(a) FESEM of VHSHRC control mix at standard conditions

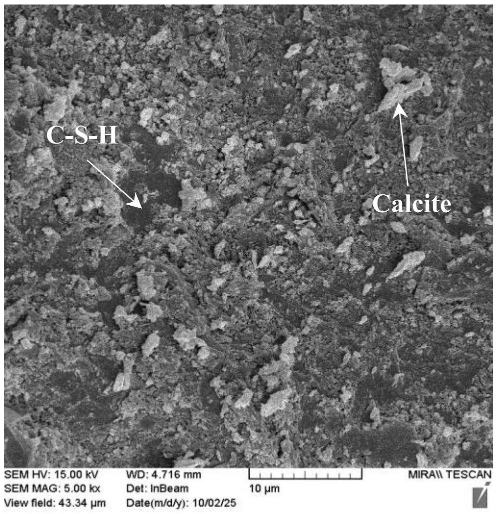

(b) FESEM of VHSHRC control mix subjected to 125°C for 6 hours

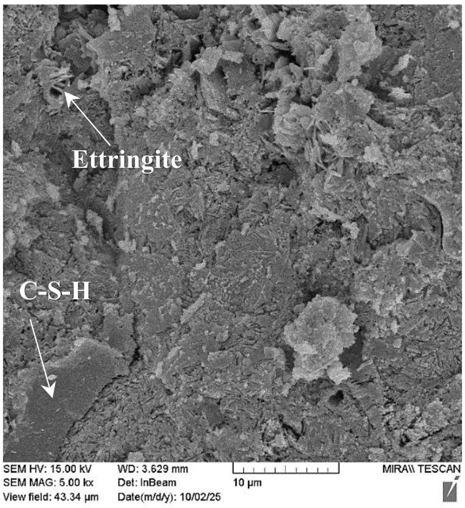

(c) FESEM of VHSHRC control mix subjected to 150°C for 6 hours

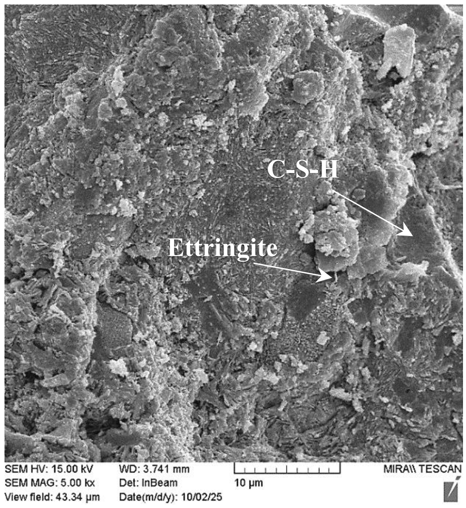

(d) FESEM of VHSHRC control mix subjected to 175°C for 6 hours

Figure 6. FESEM of VHSHRC control mix at different elevated temperatures.

Table 9: Results of the EDS test showing the main elemental weight percentage of VHSHRC under different heat exposure conditions.

Element	Weight percentage, %							
	VHSHRC control mix				VHSHRC containing 12.5% SF			
	Heating temperature, °C				Heating temperature, °C			
	20	**125**	**150**	**175**	**20**	**125**	**150**	**175**
Si	24.05	18.08	20.73	24.91	24.43	19.26	23.72	24.07
Ca	32.27	30.36	42.97	44.62	20.83	19.82	16.49	20.25
O	30.04	29.44	24.65	20.24	38.08	41.81	41.31	37.36
Al	4.25	3.55	3.21	3.61	3.11	2.89	3.12	4.15

In addition, inclusion of 12.5% SF in VHSHRC contributes to the formation of a higher amount of C–S–H by consuming portlandite via pozzolanic reaction, as shown in Figure 7a. Exposing the concrete to 125°C and 150°C leads to a slight increase in micro-cracks, as shown in Figures 7b and 7c. Furthermore, a reduction in Silicon occurs from 24.43% to 23.72%, and Calcium changes from 20.83% to 16.49% at 150°C. Conversely, with extended heating the concrete to 175°C, the weight percentage of Silicon and Calcium shows a recovery of 24.07% and 20.25%, respectively, indicating higher amount of C–S–H by secondary hydration reactions through evaporation of remaining free and combined water and filling the pores by SF which aligns with the observed increase in compressive strength compared to heated samples at 125°C and 150°C, as shown in Figure 7d.

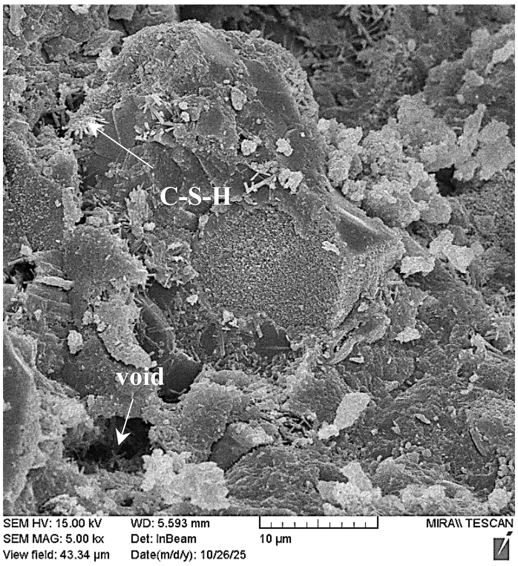

(a) FESEM of VHSHRC containing 12.5% SF

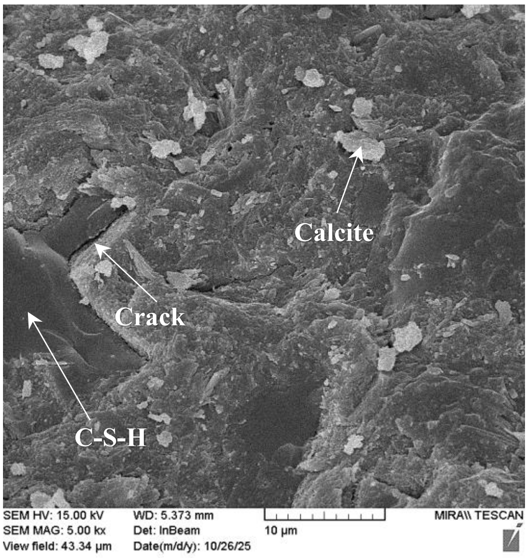

(b) FESEM of VHSHRC containing 12.5% SF exposed to 125°C for 6 hours

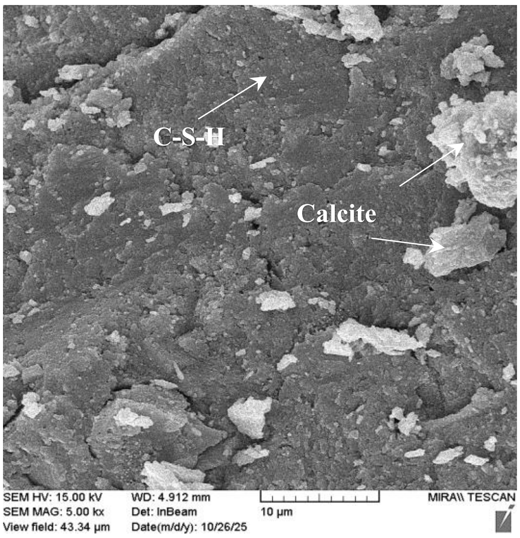

(c) FESEM of VHSHRC containing 12.5% SF exposed to 150°C for 6 hours

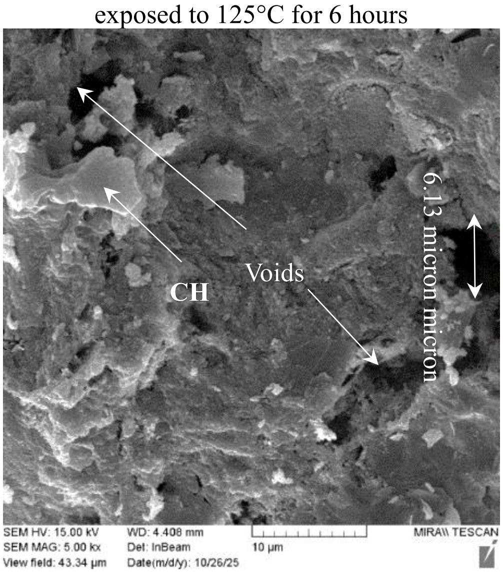

(d) FESEM of VHSHRC containing 12.5% SF exposed to 175°C for 6 hours

Figure 7. FESEM of VHSHRC containing 12.5% SF at different elevated temperatures.

5. Conclusions

This research was conducted to mitigate the impact of RAP aggregate in VHSHRC through the incorporation of SF as a partial replacement for cement. The study focused on assessing the influence of SF on some of the mechanical and non-mechanical properties of the concrete under standard conditions and at different elevated temperatures. The following conclusions can be drawn:

1. Using 12.5% of SF in VHSHRC improves the compressive strength by 3.72%, and water absorption was reduced by 32.18% at a heating temperature of 125°C. In addition, the bulk dry density decreases by 7.7% at 175°C. The reason behind the improvements is related to the high pozzolanic reaction, as revealed by microstructural analyses through increasing C-S-H gel and an increase in Silicon and Oxygen elements from FESEM and EDS tests. Besides, the high surface area of SF particles increases the water demand that produces more small pores, contributing to the reduction of the bulk dry density at all heat exposure states.
2. Inclusion of 11.5% of SF in VHSHRC reduces the water absorption up to 65.4%, 60.07%, 45.39%, and 34.19% at 20°C, 125°C, 150°C, and 175°C, respectively, due to the filling effect of ultra-fine SF particles, thereby reducing the connectivity of the capillary pores and reducing water absorption.
3. Using SF at high replacement ratios of 13% in VHSHRC does not contribute to improving the compressive and split tensile strengths of the concrete, due to the role of SF in high content, which predominantly works as a filler rather than a cementitious material in the concrete mix, resulting in reductions in strengths.

Acknowledgements
The researchers have special appreciation to the University of Sulaimani /College of Engineering/ Civil Engineering Department for their support in providing the academic environment and access to laboratory facilities throughout the conduct of this research.

Funding
This research received no specific grant from any funding agency in the public, commercial, or not-for-profit sectors.

Conflicts of Interest
The authors report no conflicts of interest.

Data Availability Statement
The data used in this study are available from the corresponding author upon reasonable request.

Institutional Review Board Statement
This study did not involve human participants or animals; therefore, ethical approval was not required.

CRediT Author Statement
Zhwan Anwar Noori: Conceptualization; Methodology; original draft preparation. Hardy Kamal Karim: supervision. Ferhad Rahim Karim: supervision, writing, and editing.
All authors have read and approved the final manuscript.

References

Abedalqader, A., Shatarat, N., Ashteyat, A., & Katkhuda, H. (2021). Influence of temperature on mechanical properties of recycled asphalt pavement aggregate and recycled coarse aggregate concrete. *Construction and Building Materials, 269*, 121285. doi: https://doi.org/10.1016/j.conbuildmat.2020.121285

Albeer, S. J., & Hassan, M. S. (2023). Silica fume modified cement-based mortar exposed to high temperatures: residual strengths and microstructure. *Journal of Engineering, 29*(07), 18-33. doi: https://doi.org/10.31026/j.eng.2023.07.02

ASTM. (2014). Standard Specification for Flow Table for Use in Tests of Hydraulic Cement *C230 / C230M–14*. West Conshohocken, PA: ASTM International. doi: 10.1520/C0230_C0230M-14

ASTM. (2018). Standard Test Methods for Chemical Analysis of Hydraulic Cement *Annual Book of ASTM Standards*. West Conshohocken, PA: ASTM International. doi: 10.1520/C0114-18

ASTM. (2019). Standard Test Methods for Time of Setting of Hydraulic Cement by Vicat Needle *C191–19*. West Conshohocken, PA: ASTM International. doi: 10.1520/C0191-19

ASTM. (2020a). ASTM C109/C109M-20: Standard Test Method for Compressive Strength of Hydraulic Cement Mortars West Conshohocken, PA: ASTM International. doi: DOI: https://doi.org/10.1520/C0109_C0109M-20

ASTM. (2020b). ASTM C496/C496M-20: Standard Test Method for Splitting Tensile Strength of Cylindrical Concrete Specimens. West Conshohocken, PA: ASTM International. doi: https://doi.org/10.1520/C0496_C0496M-23

ASTM. (2020c). Standard specification for Portland cement *ASTM C150/C150M-20*. West Conshohocken, PA: ASTM International. doi: https://doi.org/10.1520/C0150_C0150M-20

Bao, J., Zheng, R., Zhang, P., Cui, Y., Xue, S., Song, Q., & Ma, Y. (2023). Thermal resistance, water absorption and microstructure of high-strength self-compacting lightweight aggregate concrete (HSSC-LWAC) after exposure to elevated temperatures. *Construction and Building Materials, 365*, 130071. doi: https://doi.org/10.1016/j.conbuildmat.2022.130071

Behnood, A., & Ziari, H. (2008). Effects of silica fume addition and water to cement ratio on the properties of high-strength concrete after exposure to high temperatures. *Cement and Concrete Composites, 30*(2), 106-112. doi: https://doi.org/10.1016/j.cemconcomp.2007.06.003

BS. (2020). BS 1881-122:2011+A1:2020 Testing Concrete – Method for Determination of Water Absorption. London: British Standards Institution. doi: https://doi.org/10.3403/30242745

BSI. (2019). Testing hardened concrete — Part 7: Density of hardened concrete *BS EN 12390-7:2019*. London, UK: British Standards Institution. doi: https://www.bsigroup.com

Chen, J., Yuan, Y., Zhu, Q., & Duan, J. (2023). High-temperature resistance of high-strength concrete with iron tailing sand. *Journal of Building Engineering, 63*, 105544. doi: https://doi.org/10.1016/j.jobe.2022.105544

Dvorkin, L., Konkol, J., Marchuk, V., & Huts, A. (2022). Effectiveness of polymer additives in concrete for 3D concrete printing using fly ash. *Polymers, 14*(24), 5467. doi: DOI: 10.3390/polym14245467

Elmesiri, M., Ahmed, M. F., Bneni, M., ElShami, A., & Ahmad, S. (2022). Experimentally evaluation of high-performance concrete mixes used for tunnels and containing silica fume and polypropylene fiber after exposed to high temperatures. *Fracture and Structural Integrity, 16*(62), 408-425. doi: https://doi.org/10.3221/IGF-ESIS.62.28

Gernay, T., Kodur, V., Naser, M. Z., Imani, R., & Bisby, L. (2021). Concrete structures. *International Handbook of Structural Fire Engineering*, 145-188. doi: https://doi.org/10.1007/978-3-030-77123-2_6

Ghandehari, M., Behnood, A., & Khanzadi, M. (2010). Residual mechanical properties of high-strength concretes after exposure to elevated temperatures. *Journal of Materials in Civil Engineering, 22*(1), 59-64. doi: https://doi.org/10.1061/(ASCE)0899-1561(2010)22:1(59)

Hilal, A. A. (2016). Microstructure of concrete. *High performance concrete technology and applications, 5*. doi: DOI: 10.5772/64574

Ibrahim, K. (2016). The effect of heat on the compressive strength of silica fume concrete (SFC). *J. Mech. Civil Eng., 13*(3), 24-28. doi: DOI: 10.9790/1684-1303042428

Jaawani, S., Franco, A., De Luca, G., Coppola, O., & Bonati, A. (2021). Limitations on the use of recycled asphalt pavement in structural concrete. *Applied Sciences, 11*(22), 10901. doi: https://doi.org/10.3390/app112210901

Karim, F. R. (2024). *Strengthening a thin crust of lightweight pumice aggregate in low strength concrete for tensile and compressive strengths* Paper presented at the The 3rd International Conference on Engineering and innovative Technology, Erbil. doi: https://doi.org/10.31972/iceit2024.063

Knight, K. A., Cunningham, P. R., & Miller, S. A. (2023). Optimizing supplementary cementitious material replacement to minimize the environmental impacts of concrete. *Cement and Concrete Composites, 139*, 105049. doi: https://doi.org/10.1016/j.cemconcomp.2023.105049

Kulkarni, V. R. (2016). High performance concrete for high-rise buildings: Some crucial issues. *International Journal of Research in Engineering and Technology*, 26-33.

Kumar, R., Verma, M., & Dev, N. (2024). Analysis of PCE-based Superplasticiser for the Different Types of Cement using Marsh Cone Test. doi: doi:10.5109/7183337

Mehta, P. K., & Monteiro, P. (2014). *Concrete : microstructure, properties, and materials* (4th ed ed.): McGraw-Hill. doi: https://cir.nii.ac.jp/crid/1130000797867624064

Nadeem, A., Memon, S. A., & Lo, T. Y. (2014). The performance of fly ash and metakaolin concrete at elevated temperatures. *Construction and Building Materials, 62*, 67-76. doi: https://doi.org/10.1016/j.conbuildmat.2014.02.073

Noori, Z. A., Karim, F. R., & Karim, H. K. (2025). Influence of Recycled Asphalt Pavement Aggregate on the Mechanical Properties of Very-High Strength Heat-Resistant Concrete. *CONSTRUCTION, 5*(2). doi: DOI: https://doi.org/10.15282/construction.v5i2.12758

Noori, Z. A., Karim, F. R., & Karim, H. K. (2026). Improvement of the Brittleness and Drying shrinkage in Very High Strength Concrete Incorporating Micro Metakaolin. *Smart and Green Materials, 3*(1), 1-17. doi: https://doi.org/10.70028/sgm.v3i1.77

Otakulov, B. A., Abdullayev, I. A., & Toshpulatov, J. O. O. (2021). IMPORTANCE OF HEAT-RESISTANT CONCRETE IN CONSTRUCTION. *Scientific progress, 2*(6), 1613-1616.

Roussel, N. (2006). A thixotropy model for fresh fluid concretes: Theory, validation and applications. *Cement and Concrete Research, 36*(10), 1797-1806. doi: https://doi.org/10.1016/j.cemconres.2006.05.025

Tanash, A. O., Bakar, B. A., Muthusamy, K., & Biajawi, M. I. A. (2024). Effect of elevated temperature on mechanical properties of normal strength concrete: An overview. *Materials Today: Proceedings, 107*, 152-157. doi: https://doi.org/10.1016/j.matpr.2023.09.053

Yang, I.-H., & Hwang, C.-S. (2017). An Experimental Study of Mechanical Properties of High-strength Concrete. *Journal of the Korea institute for structural maintenance and inspection, 21*(6), 206-215.

Zia, P., Ahmad, S. H., Leming, M. L., Schemmel, J., & Elliott, R. (1993). Mechanical behavior of high performance concretes, volume 5: Very high strength concrete.